A Low-Cost and Smart IMU Tool for Tracking Construction Activities

X. Yang[a,b,*], F. Wang[a], X. Zhai[a], H. Li[b], Y. Yu[b], and X. Luo[b]

[a]School of Civil Engineering, Harbin Institute of Technology, Harbin, China
[b]Department of Building and Real Estate, The Hong Kong Polytechnic University, Hong Kong
E-mail: xincong.yang@outlook.com, fl-wang@hit.edu.cn, xmzhai@hit.edu.cn, yt.yu@connect.polyu.hk, heng.li@polyu.edu.hk, eric.xiaochun.luo@polyu.edu.hk

Abstract –

Real-time activity monitoring is becoming one of the most significant technologies on construction sites because it can be applied to a variety of management problems, such as productivity formula and safety monitoring. However, current monitoring technologies are limited to recognizing postures in an ideal environment rather than dealing with the ambient occlusion and people-intensive situations on real construction sites. Therefore, this study develops a low-cost, non-intrusion and portable tool system in order to trace and track construction activities on complex and crowed construction sites. This system is composed of wireless sensors and a smart algorithm. Each sensor consists of an inertial measurement unit, a communication sensor (bluetooth low energy sensor) and several environmental sensors, which broadcasts the identification, acceleration, palstance and environmental measurements at a constant frequency. Since the dimension of the sensor is only 20 x 15 x 2 mm, it can be easily attached or screwed on to the hand tools as well as integrated with power tools. When a laptop or cell phone receives from these sensors, the construction activities are derived by the artificial intelligence algorithm in a timely manner, providing an visual posture monitoring as well as an automatic record of project progress. In the end, practical experiments of a concrete vibrator and a hammer prove the feasibility and effectiveness of the proposed IMU-based tool tracing and tracking system.

Keywords –

Inertial measurement unit; Construction tools; Activity recognition; Non-intrusive; Low-cost

1 Introduction

Construction is a typical labor-intensive industry that a variety of construction assignments are accomplished manually, such as wood formwork, bar bending and tying, concrete pouring, etc. Therefore, the on-site construction activity is one of the critical resources contributing to the construction project performance, and its effective control and management is always considered as a key to success [1]. By tracking workers-on-foot and construction heavy equipment, near-misses, collisions and safety risks can be prevented and alleviated [2], dangerous and awkward postures can be detected and alarmed [3], productivity can be measured in a timely and quantitative manner [4-6], etc.

The main obstacle for automated construction activity control and management is the real-time activity tracking. State-of-the-art technologies, including computer vision, wearable sensor, etc., which are available for on-site motion tracking, are emerging; however, the installation or monitoring process is intrusive and the effectiveness is seriously affected by complicated environment, such as none-line-of-sight effect due to ambient occlusions and multipath effect by signal reflection.

The purpose of the present study is to develop a smart and low-cost IMU-based tool system and test the feasibility for on-site activity tracking. The research introduced the novel concept and established the framework of the proposed system at first, developed a general prototype and an effective algorithm for construction works using cyclic patterns, and finally, conducted a pilot study to validate the system [7].

2 Background

The conventional way to monitor construction activities is human inspection, which is still the popular at the present time. An inspector roams around the site at regular intervals, the records the observation and draws a daily or weekly report. Once awkward or dangerous postures are recognized, the inspector send alarms and prevent further damage to the health and safety of workers. This is a commendable achievement, but it requires full time observation, which is impossible and inefficiency for such a large field as construction site [8].

In the recent times, cutting-edge sensors are introduced to evaluate the spatial-temporal activities in the construction industry by attaching inertial and biomechanical sensors on human body segments [9]. The earliest instruments for linear posture detection are tapes and goniometer, and further progress is the advent of electromyographic devices (EMG) that using the muscle strength to access the movement and rotation. However, these devices are only used in clinical environments as they are tedious and intrusive to deploy [10]. With the emergence and development of micro-electro-mechanical system (MEMS), the device measuring the inertial properties of objects becomes small while the accuracy, robustness and quick response are improved dramatically, which is called inertial measurement unit (IMU). Nowadays, commercial IMU is usually made up of a tri-axis gyroscope and a tri-axis accelerometer (6-axis IMU), and a tri-axis magnetometer (9-axis IMU), enabling the measurement of acceleration, angular velocity, and magnetic field [11]. Scholars have applied this technology to detect awkward postures to prevent musculoskeletal disorders [3, 12, 13], near-misses and hazards are also recognized automatically and analyzed to assess the potential risks [14].

Another popular way to monitor construction activities is by computer vision, which can be briefly categorized into three types according to their instruments: monocular, binocular and depth cameras [1]. Compared with sensor-based activity monitoring, CV-based methods are visual and insightful, enabling to record various information, not only workers but also associated contexts [15]. At the beginning, computer vision is used to localize construction resources, including manpower, excavators, cranes, etc., providing a picture of space use on sites [16], predicting the proximity conflicts [17, 18]. After that, with the advent of deep learning techniques, motion recognition and tracking is available that specific body skeleton can be extracted from images or videos. Scholars then transform the technology into monitoring construction activities [19-21]. Risky and dangerous behaviors, such as falling from heights, not wearing a hat or personal protective equipment, hazardous materials, etc. are identified by cameras.

The pros of sensor-based human posture detection contain direct and simple measuring principle, high accuracy and frequency, as well as low latency and cost. However, the cons of this detection are also distinct that the deployment is tedious and intrusive as people are prone to suffer from discomfort and motion restriction by the attached sensors. What’s more, the privacy issue of monitoring the personal data also exacerbates the problem. On the other hand, the considerable advantages CV-based human posture detection consist of non-intrusion into normal construction activities, easy deployment, remote monitoring, tremendous potential for artificial intelligence. Nevertheless, some disadvantages hinder the wide applications in practice. A primary disadvantage of CV-based human posture detection is the legal issue of intrusion of privacy that employees may object to being filmed under constant surveillance. Another disadvantage is the cost. As construction sites are always huge, high-resolution cameras are required, added by the instruments for transmission, compression and storage, it is expensive to purchase and keep the detection algorithms upgraded all the time. The third disadvantage is the non-line-of-sight (NLoS) effect due to ambient occlusions that CV-based detection performs badly without direct observations. What’s more, the illumination and transparency of exposed environment also have an adverse impact on the detection. Other disadvantages, such as low accuracy and high latency or frame loss, weaken the applicable ability in construction industry as well.

Either sensor-based or CV-based human posture detection has exposed their weaknesses in literature and practice. This research therefore proposes a novel approach that leveraging the location and posture of a hand tool or power tool to detect the corresponding human postures by a single MEMS-IMU [22, 23]. This creative conceptual approach is not only a positive solution of personnel concerns and privacy that employees are not working under immediate surveillance, but also a non-intrusive and marker-less solution of human posture detection.

3 Framework for tracking construction activities by tools

This is an insightful conception that the way human beings make and use tools is perhaps what sets us apart more than anything else. In turn, tools also have positive impacts on our evolution. Workers in modern industries are always carry out their jobs with the assistance of valuable tools.

Construction is a typical labor-intensive industry that a variety of construction assignments are accomplished manually. To improve the productivity and ensure the safety, diverse tools are designed and adopted on constriction sites, containing hand tools (tape measure, torpedo level, screwdriver, wrench, trowel, hammer, coping saw, etc.), as well as power tools (circular saw, drill. jig saw, orbit sander, angle grinder, etc.) in Figure 1.

Figure 1. Common hand and power tools can be integrated with an IMU sensor

Thus, for these kinds of jobs using various assistant tools, the motions of tools apparently describe the detailed process of construction activities. For example, the trajectory of concrete vibrator suggests the area of concrete consolidation after pouring; the angular rotation of screwdriver indicates the effects of workers on the connection of reinforcement bars. The data of tools therefore not only suggest the status of construction activities, but also work as an event data recorder that record the associated information during specific events. When an accident happens, the information can be collected for analysis, to identify the status before, during and after the accident.

The schematic model for this tool-based construction activity monitoring is illustrated in Figure 2. To monitor the construction activities, manual assignments are transformed into tool motions at first. For example, the acceleration of tools indicates the workload at the construction stage; the velocity and angular velocity (palstance) exposes the mobile characteristics of workers; and position, rotation of tools provides a relative reference of the postures of workers. Then the construction regulations, standards, or codes are represented by tool rules. By comparing the tool data and these rules, it is a quantitative way to determine whether the actual construction activity is in conformity to the existing strict regulations [24].

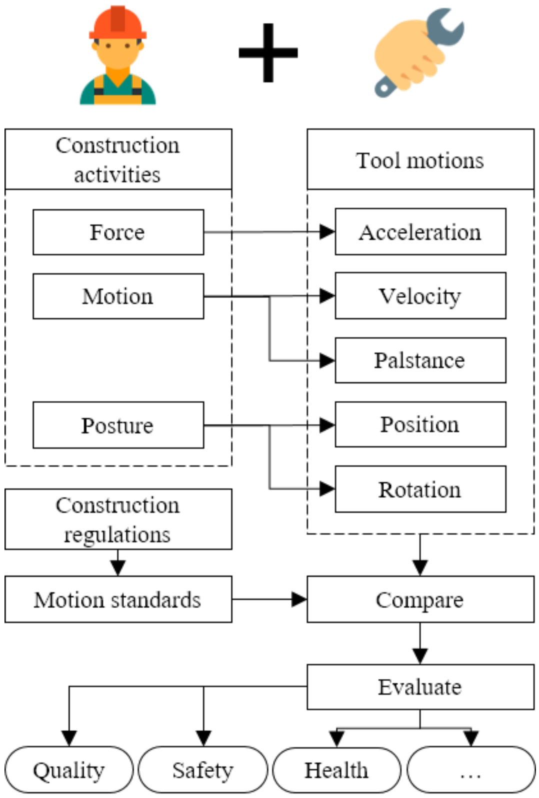

Figure 2. Schematic model for the IMU tool system

4 Data collection method

Various methods can be considered for the implementation of the framework for tracking the construction activities on-site. Among the current cutting-edge technologies, electro-mechanical system inertial measurement units (MEMS-IMUs) are economic and easy-handling.

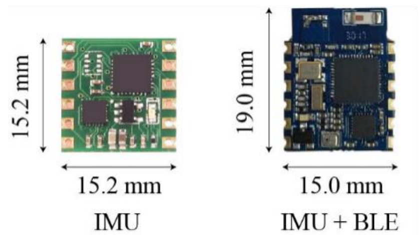

Figure 3. IMU and IMU+BLE sensors to collect tool data

As shown in Figure 3, the sensors are quite small and light, which can be integrated with power tools or installed on hand tools. This simple deployment ensures the non-intrusion during the construction stage.

These sensors are able to collect acceleration and angular velocity as a tri-accelerometer and a tri-gyroscope are imbedded in. Therefore, the task diagram of IMU sensors is described in Figure 4. The IMU starts with measuring acceleration and angular velocity, and the calibrate each other according to the earth model. The adjusted acceleration is integral to produce velocity, and integral twice to generate displacement. Meanwhile the calibrated angular velocity is then integral to obtain the rotation and orientation at each time interval. By differential operation, the angular velocity can extract the angular acceleration as well. Noted that the magnetometer is more sensitive to tiny changes in direction, 9-axis is more common in applications as the measurement of magnetic field improve the accuracy significantly by calibrating at a high frequency.

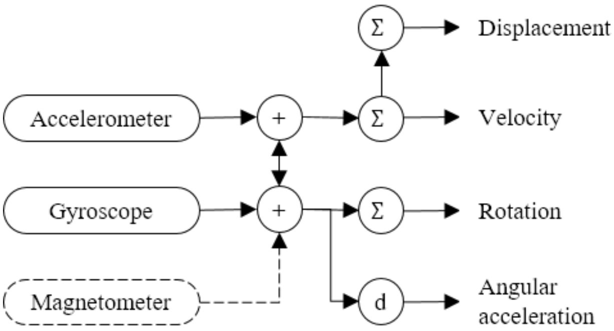

Figure 4. Task diagram of IMUs

The kinematics of a rigid body like a tool is composed of translation and rotation. This research only focuses on the rotation component as it produces considerable impacts on bar connections. Although the initial data collected by MEMS-IMU is in Euler angle form, here the orientation is represented in quaternion form which is simple and efficient in transforming computation. Thus, a rotation around axis $\boldsymbol{n}$ with an angle of θ is represented by

$$\boldsymbol{Q} = \left[\cos\left(\frac{\theta}{2}\right), \sin\left(\frac{\theta}{2}\right)\boldsymbol{n}\right] = [q_0, q_1, q_2, q_3] \tag{1}$$

While the orientation $\boldsymbol{R}$ is denoted by

$$\boldsymbol{R} = [0, \boldsymbol{r}] = [0, r_1, r_2, r_3] \tag{2}$$

The corresponding differential function is written by

$$\frac{\mathrm{d}\boldsymbol{Q}}{\mathrm{d}t} = \frac{1}{2}\boldsymbol{Q} \otimes \boldsymbol{\omega}_{\mathrm{nb}}^{\mathrm{b}} \tag{3}$$

where $\boldsymbol{\omega}_{\mathrm{nb}}^{\mathrm{b}} = [\omega_x \quad \omega_y \quad \omega_z]^{\mathrm{T}}$, refers to the angular velocity of each axis. And the matrix form of formula can be represented by

$$\begin{bmatrix} \dot{q_0} \\ \dot{q_1} \\ \dot{q_2} \\ \dot{q_3} \end{bmatrix} = \begin{bmatrix} 0 & -\omega_x & -\omega_y & -\omega_z \\ \omega_x & 0 & \omega_z & -\omega_y \\ \omega_y & -\omega_z & 0 & \omega_x \\ \omega_z & \omega_y & -\omega_x & 0 \end{bmatrix} \begin{bmatrix} q_0 \\ q_1 \\ q_2 \\ q_3 \end{bmatrix} \tag{4}$$

As the MEMS-IMU measures the angular velocity at a constant frequency, the iteration formulation is

$$\boldsymbol{Q}(t+1) = (\boldsymbol{I}\cos\frac{2\Delta\theta}{2} + \Delta\boldsymbol{\Omega}\frac{\sin\frac{2\Delta\theta}{2}}{\Delta\theta})\boldsymbol{Q}(t) \tag{5}$$

where $\Delta\boldsymbol{\Omega} = \begin{bmatrix} 0 & -\Delta\theta_x & -\Delta\theta_y & -\Delta\theta_z \\ \Delta\theta_x & 0 & \Delta\theta_z & -\Delta\theta_y \\ \Delta\theta_y & -\Delta\theta_z & 0 & \Delta\theta_x \\ \Delta\theta_z & \Delta\theta_y & -\Delta\theta_x & 0 \end{bmatrix}$, refers to the direct output of MEMS-IMU, $\Delta\theta = \sqrt{\Delta\theta_x^2 + \Delta\theta_y^2 + \Delta\theta_z^2}$ is the total changes of angular velocity.

The initial quaternion is determined be the transformation matrix from the earth frame to the sensor body frame, which is represented by

$$\begin{gathered} \boldsymbol{C}_{\mathrm{n}}^{\mathrm{b}} = [\boldsymbol{c_1}, \boldsymbol{c_2}, \boldsymbol{c_3}] \\ \boldsymbol{c_1} = \begin{bmatrix} q_0^2 + q_1^2 - q_2^2 - q_3^2 \\ 2(q_1q_2 + q_0q_3) \\ 2(q_1q_3 - q_0q_2) \end{bmatrix} \\ \boldsymbol{c_2} = \begin{bmatrix} 2(q_1q_2 - q_0q_3) \\ q_0^2 - q_1^2 + q_2^2 - q_3^2 \\ 2(q_2q_3 + q_0q_1) \end{bmatrix} \\ \boldsymbol{c_3} = \begin{bmatrix} 2(q_1q_3 + q_0) \\ 2(q_2q_3 - q_0q_1) \\ q_0^2 - q_1^2 - q_2^2 + q_3^2 \end{bmatrix} \end{gathered} \tag{6}$$

At the same time, $\|\boldsymbol{Q}\| = 1$ that each quaternion of rotation and orientation is normalized.

Although the integral approach appears to be accurate in theory, random noise, signal bias, etc. accumulates overtime. To improve the robustness and accuracy of rotation measurement, acceleration and magnetic field data collected by accelerometer and magnetometer are fused to orientation estimation by gyroscopes as well. Given a specific construction field, the direction of gravity and magnetic field are known. An orientation of the sensor frame relative to the earth frame is therefore calculated by comparing the measurement by gyroscope and by accelerometer and magnetometer.

If the rotation quaternion relates the earth frame to the sensor body frame is denoted by $\boldsymbol{q}_{\mathrm{e}}^{\mathrm{b}}$, the expected measurement of acceleration and magnetic field in the earth frame is denoted by $\boldsymbol{d}^{\mathrm{e}}$, meanwhile these in the sensor body frame measured in real-time is represented by $\boldsymbol{s}^{\mathrm{b}}$. The fusion of acceleration data and magnetic field data is modeled as an optimization problem. The objective function is

$$f\left(\boldsymbol{q}_{\mathrm{e}}^{\mathrm{b}}, \boldsymbol{d}^{\mathrm{e}}, \boldsymbol{s}^{\mathrm{e}}\right) = \boldsymbol{q}_{\mathrm{e}}^{\mathrm{b}*} \otimes \boldsymbol{d}^{\mathrm{e}} \otimes \boldsymbol{q}_{\mathrm{e}}^{\mathrm{b}} - \boldsymbol{s}^{\mathrm{b}} \tag{7}$$

To approximate to the minimum of the objective function, the corresponding gradient of the objective function is written by

$$\nabla f(\boldsymbol{q}_{\mathrm{e}}^{\mathrm{b}}, \boldsymbol{d}^{\mathrm{e}}, \boldsymbol{s}^{\mathrm{e}}) = \boldsymbol{J}^{\mathrm{T}}(\boldsymbol{q}_{\mathrm{e}}^{\mathrm{b}}, \boldsymbol{d}^{\mathrm{e}}) f(\boldsymbol{q}_{\mathrm{e}}^{\mathrm{b}}, \boldsymbol{d}^{\mathrm{e}}, \boldsymbol{s}^{\mathrm{e}}) \tag{8}$$

where $\boldsymbol{J}$ is the Jacobian matrix.

For acceleration data,

$$\boldsymbol{s}^{\mathrm{e}} = [0 \quad 0 \quad 0 \quad 1] \tag{9}$$

$$f(\boldsymbol{q}_{\mathrm{e}}^{\mathrm{b}}, \boldsymbol{a}^{\mathrm{e}}, \boldsymbol{s}^{\mathrm{e}}) = \begin{bmatrix} 2(q_1q_3 - q_0q_2) - a_x \\ 2(q_0q_1 + q_2q_3) - a_y \\ (1 - 2q_1^2 - 2q_2^2) - a_z \end{bmatrix} \tag{10}$$

$$\boldsymbol{J}(\boldsymbol{q}_{\mathrm{e}}^{\mathrm{b}}, \boldsymbol{a}^{\mathrm{e}}) = \begin{bmatrix} -2q_2 & 2q_3 & -2q_0 & 2q_1 \\ 2q_1 & 2q_0 & 2q_3 & 2q_2 \\ 0 & -4q_1 & -4q_2 & 0 \end{bmatrix} \tag{11}$$

For magnetic field,

$$\boldsymbol{s}^{\mathrm{e}} = [0 \quad s_x \quad 0 \quad s_z] \tag{12}$$

$$f(\boldsymbol{q}_{\mathrm{e}}^{\mathrm{b}}, \boldsymbol{m}^{\mathrm{e}}, \boldsymbol{s}^{\mathrm{e}}) = \begin{bmatrix} 2s_x(0.5 - q_2^2 - q_3^2) + 2s_z(q_1q_3 - q_0q_2) - m_x \\ 2s_x(q_1q_2 - q_0q_3) + 2s_z(q_0q_1 + q_2q_3) - m_y \\ 2s_x(q_0q_2 + q_1q_3) + 2s_z(0.5 - q_1^2 - q_2^2) - m_z \end{bmatrix} \tag{13}$$

$$\begin{gathered} \boldsymbol{J}(\boldsymbol{q}_{\mathrm{e}}^{\mathrm{b}}, \boldsymbol{a}^{\mathrm{e}}) = [\boldsymbol{J_1}, \boldsymbol{J_2}, \boldsymbol{J_3}, \boldsymbol{J_4}] \\ \boldsymbol{J_1} = \begin{bmatrix} -2s_zq_3 \\ -2s_xq_3 + 2s_zq_1 \\ 2s_xq_2 \end{bmatrix} \\ \boldsymbol{J_2} = \begin{bmatrix} 2s_zq_3 \\ 2s_xq_2 + 2s_zq_0 \\ 2s_xq_3 - 4s_zq_1 \end{bmatrix} \\ \boldsymbol{J_3} = \begin{bmatrix} -4s_xq_2 - 2s_zq_0 \\ 2s_xq_1 + 2s_zq_3 \\ 2s_xq_0 - 4s_zq_2 \end{bmatrix} \\ \boldsymbol{J_4} = \begin{bmatrix} -4s_xq_3 + 2s_zq_1 \\ -2s_xq_0 + 2s_zq_2 \\ 2s_xq_1 \end{bmatrix} \end{gathered} \tag{14}$$

In this research, acceleration, angular velocity and magnetic field data are available, 9-axis MEMS-IMU algorithms is therefore applied to fuse and combine these data for compensating distortion, filtering erroneous data and smoothing. The fundamental way to accomplish this goal is Kalman filter.

Consider the spatial-temporal characteristics of a construction tool is a state vector that contains a series of variables. The model assumes that the true state at current time t is evolved from the state at the previous time t - 1. This discrete-time linear stationary model without control loop can be represented by

$$\boldsymbol{x}_t = \boldsymbol{\Phi}\boldsymbol{x}_{t-1} + \boldsymbol{\Gamma}\mathbf{w}_{t-1} \tag{15}$$

where x is the state vector, $\boldsymbol{\Phi}$ refers to the state transition matrix, $\boldsymbol{\Gamma}$ is the control matrix of noises, $\mathbf{w} \sim \boldsymbol{\mathcal{N}}(\mathbf{0}, \mathbf{W}_{\mathrm{t}})$ represents the process noise that is assumed to be generated from a zero mean multivariate normal distribution $\boldsymbol{\mathcal{N}}$ with covariance $\mathbf{W}_{\mathrm{t}}$.

Concurrently, the measurement process is:

$$\boldsymbol{z}_t = \mathbf{H}\boldsymbol{x}_t + \mathbf{v}_{\mathrm{t}} \tag{16}$$

where H is the observation matrix and $\mathbf{v} \sim \boldsymbol{\mathcal{N}}(\mathbf{0}, \mathbf{V}_{\mathrm{t}})$ is the observation noise that drawn from a zero mean Gaussian distribution $\boldsymbol{\mathcal{N}}$ with covariance $\mathbf{V}_{\mathrm{t}}$.

5 Pilot study and results

As shown in Figure 5, IMU sensors can be deployed on the surface of a wrench, a hammer, etc. By tight connection, the data collected is according to the location of sensors, that is to say, the crucial axis for analysis is determined by the position and relation between sensor deployment and the core motion space.

Figure 5. Deployment of IMU sensors

The MEMS-IMU sensor tested here required extra battery support, and the chip is named JY901. The weight is 40 g and the size is less than 2 cm^2, almost non-intrusive when used.

Assume a wrench is adopted to apply torque to turn a screw for connection. Wireless MEMS-IMU is the device collecting the data of the combination wrench, providing a quantitative assessment of turning. In addition, a rubber mallet is also tested to conduct a wood work, requiring a softened strike with a positive drive.

In Figure 6, the curves of raw data revealed the turning process by a wrench rotating around y-axis. It could be seen that the turning job appears to be cyclic in much the same way as a wave with various frequencies. By integral operation, the rotation angle of turning process was shown in Figure 7. The cyclic pattern was more apparent that each cycle ranged from 0 to 90 degree at the begging time for applying torque, and then decreased to the initial position for the next cycle. In this experiment, 22 cycles were counted and the total rotation angle of turning was around 1442 degree, that means the screw has been turned for 4 circles. While the actual rotation was 1620 degree, and the relative measurement error was 10.99%.

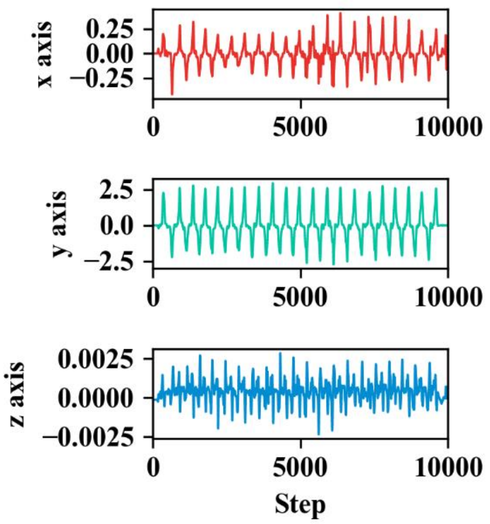

Figure 6. Angular velocity of turning collected by MEMS-IMU

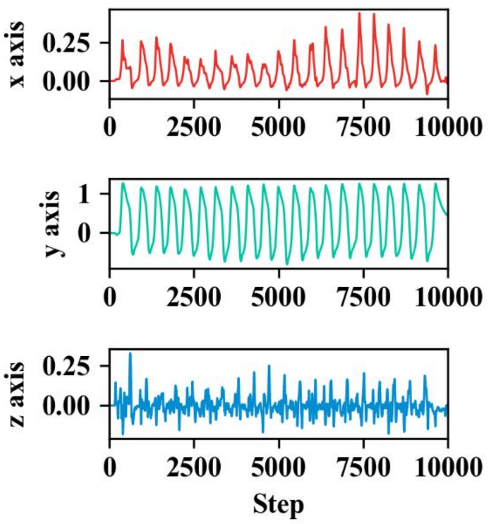

Figure 7. Rotation of turning collected by MEMS-IMU

On the other hand, the angular velocity of hammering process in Figure 8 exposed another kind of cyclic patterns. Here, x-axis was the rotation axis that the rubber mallet was held to hit on the objective panel. The extreme values of palstance were much higher than those of turning process. At the same time, the rotation angle of hammering was also larger as shown in Figure 9. The process begun with hanging on the mallet at the rotation angle of zero, then fell down as the rotation angle raised up to around 90 degrees. However, the measurement of highest rotation angles in each cycle was not accurate that the obtained value was more than 143 degrees. The error was unacceptable at this moment, which required to be improved in the future.

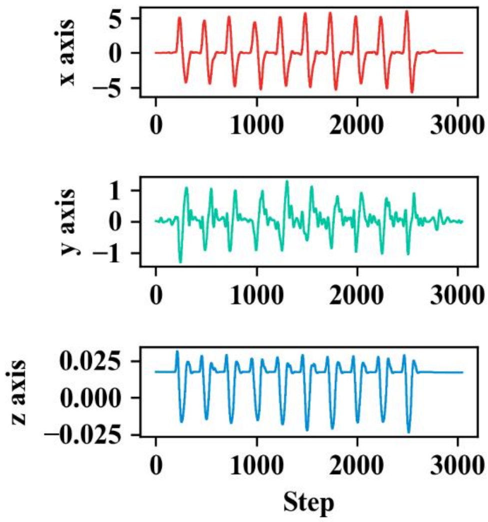

Figure 8. Angular velocity of hammering collected by MEMS-IMU

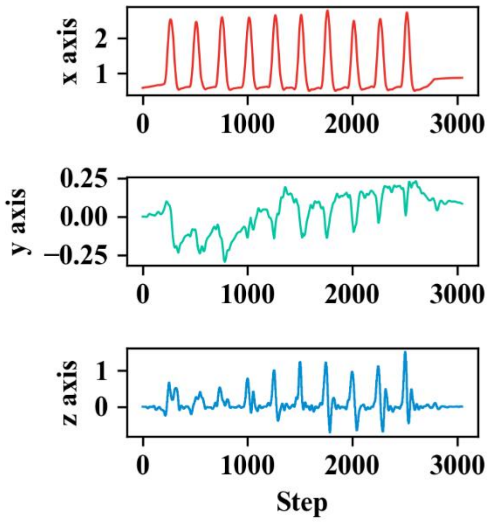

Figure 9. Rotation of hammering collected by MEMS-IMU

By comparing the different cyclic patterns from these two preliminary experiments, the extracted raw data clearly revealed the spatial-temporal characteristics of the different construction activities. Although the data was not so accurate because the current MEMS-IMU algorithm enlarged the cumulative errors over time, these two pilot studies have shown the potential of the proposed IMU-based tool system for monitoring the construction activities in a timely and automated manner.

6 Conclusion

This study proposed a feasible solution to monitor the construction activities without intrusions by collecting and analyzing the IMU data of hand tools used in the construction processes. Two simple experiments validated the novel concept and the preliminary framework. However, further developments were required in the future research, containing the reduction of random errors and cumulative errors and the pattern recognition for various tools and activities.

References

[1] Lee, Y.-J. and M.-W. Park, 3D tracking of multiple onsite workers based on stereo vision. *Automation in Construction*, 2019. 98: p. 146-159.

[2] Golovina, O., J. Teizer, and N. Pradhananga, Heat map generation for predictive safety planning: Preventing struck-by and near miss interactions between workers-on-foot and construction equipment. *Automation in Construction*, 2016. 71: p. 99-115.

[3] Chen, J., J. Qiu, and C. Ahn, Construction worker's awkward posture recognition through supervised motion tensor decomposition. *Automation in Construction*, 2017. 77: p. 67-81.

[4] Hui, L., M.-W. Park, and I. Brilakis, Automated Brick Counting for Facade Construction Progress Estimation. *Journal of Computing in Civil Engineering*, 2015. 29(6): p. 04014091.

[5] Sacks, R., R. Navon, and E. Goldschmidt, Building project model support for automated labor monitoring. *Journal of computing in civil engineering*, 2003. 17(1): p. 19-27.

[6] Navon, R. and E. Goldschmidt, Can labor inputs be measured and controlled automatically? *Journal of Construction Engineering and Management*, 2003. 129(4): p. 437-445.

[7] Hajdasz, M., Flexible management of repetitive construction processes by an intelligent support system. *Expert Systems with Applications*, 2014. 41(4): p. 962-973.

[8] Navon, R. and R. Sacks, Assessing research issues in automated project performance control (APPC). *Automation in Construction*, 2007. 16(4): p. 474-484.

[9] Luinge, H.J. and P.H. Veltink, Measuring orientation of human body segments using miniature gyroscopes and accelerometers. *Medical and Biological Engineering and Computing*, 2005. 43(2): p. 273-282.

[10] Valero, E., et al., Musculoskeletal disorders in construction: A review and a novel system for activity tracking with body area network. *Applied Ergonomics*, 2016. 54: p. 120-130.

[11] Seel, T., J. Raisch, and T. Schauer, IMU-based joint angle measurement for gait analysis. *Sensors*, 2014. 14(4): p. 6891-6909.

[12] Valero, E., et al., Analysis of construction trade worker body motions using a wearable and wireless motion sensor network. *Automation in Construction*, 2017. 83: p. 48-55.

[13] Yan, X., et al., Wearable IMU-based real-time motion warning system for construction workers' musculoskeletal disorders prevention. *Automation in Construction*, 2017. 74: p. 2-11.

[14] Jebelli, H., C.R. Ahn, and T.L. Stentz, Fall risk analysis of construction workers using inertial measurement units: Validating the usefulness of the postural stability metrics in construction. *Safety Science*, 2016. 84: p. 161-170.

[15] Fang, Q., et al., Computer vision aided inspection on falling prevention measures for steeplejacks in an aerial environment. *Automation in Construction*, 2018. 93: p. 148-164.

[16] Tomé, A., et al., Space–use analysis through computer vision. *Automation in Construction*, 2015. 57: p. 80-97.

[17] Kim, D., et al., Remote proximity monitoring between mobile construction resources using camera-mounted UAVs. *Automation in Construction*, 2019. 99: p. 168-182.

[18] Akinci, B., et al., Formalization and automation of time-space conflict analysis. *Journal of Computing in Civil Engineering*, 2002. 16(2): p. 124-134.

[19] Yang, J., Z. Shi, and Z. Wu, Vision-based action recognition of construction workers using dense trajectories. *Advanced Engineering Informatics*, 2016. 30(3): p. 327-336.

[20] Seo, J., et al., Computer vision techniques for construction safety and health monitoring. *Advanced Engineering Informatics*, 2015. 29(2): p. 239-251.

[21] Gong, J., C.H. Caldas, and C. Gordon, Learning and classifying actions of construction workers and equipment using Bag-of-Video-Feature-Words and Bayesian network models. *Advanced Engineering Informatics*, 2011. 25(4): p. 771-782.

[22] Li, H., et al., Automated classification of construction site hazard zones by crowd-sourced integrated density maps. *Automation in Construction*, 2017. 81: p. 328-339.

[23] Yang, X., et al., Location-based measurement and visualization for interdependence network on construction sites. *Advanced Engineering Informatics*, 2017. 34: p. 36-45.

[24] Eastman, C., et al., Automatic rule-based checking of building designs. *Automation in construction*, 2009. 18(8): p. 1011-1033.